JOURNAL OF MATERIALS SCIENCE 19 (1984) 263–269

Creep behaviour of a 25wt % Cr–20wt % Ni austenitic stainless steel doped with antimony

T. YAMANE, N. GENMA
Department of Materials Science and Engineering, Osaka University, Suita 565, Japan

Y. TAKAHASHI
Department of Welding Engineering, Osaka University, Suita 565, Japan

The effect of antimony on the steady state creep rates, $\dot{\epsilon}_s$, of a 25 wt % Cr–20 wt % Ni austenitic stainless steel with 0.005 wt % C is studied. The effect on vacancy viscous creep (Coble creep) is shown to be different to that on dislocation creep (power law creep). The effect on Coble creep is particularly striking. The threshold stress is significantly increased by antimony additions.

1. Introduction

Impurities in a polycrystalline metal can have an influence on the mechanical properties if they segregate to grain boundaries [1–4]. Antimony is an element of this type, in particular for steels which include nickel and chromium [5, 6].

The segregation to grain boundaries is particularly important in determining the creep behaviour, because boundaries act as sources and sinks for matrix dislocations and vacancies, which are necessary for dislocation creep and diffusion creep, respectively [7, 8]. Amongst the possibilities, the following categories may be listed.

(i) The threshold stress, σ_t, for diffusion creep can be increased, i.e. the segregation can make it possible to observe Bingham behaviour [9–12].

(ii) The generation and annihilation of matrix dislocations at grain boundaries can be enhanced or inhibited [7, 8].

(iii) Subgrain boundaries can be stabilized by impurities [13, 14].

There is little information on how the steady state creep rates of a 25 wt % Cr–20 wt % Ni austenitic stainless steel are affected by small additions of antimony. In the present paper, the steady state creep behaviour of such an alloy is experimentally studied with a view to assessing segregation effects.

2. Creep deformation mechanisms and experimental conditions

We have previously reported upon the creep behaviours of a precipitate-free 25 wt % Cr–20 wt % Ni austenitic stainless steel without antimony additions [15, 16]. These studies provided a basis for the present study of the segregation-effects of (i) to (iii).

Fig. 1 shows a deformation mechanism map for the steady state creep of the steel. This map is identical to the diagram in our previous papers. Here, σ is the creep stress, G the shear modulus, T the creep temperature in Kelvin, T_m the melting temperature (the solidus temperature) in degrees Kelvin, d the grain size, and b the Burgers vector. Domains G_1 and G_2, represent "dislocation-glide". G_1 is "viscous glide", and G_2 is "jerky glide". Three domains of R_1, R_2 and R_3 represent recovery controlled dislocation creep [17], but each show different features. Domain R_1 is predominantly controlled by grain boundaries, i.e. the process of the generation and annihilation of matrix dislocations at grain boundaries. On the other hand, domain R_3 is strongly associated with the formation of dislocation substructure, which is considered to be metastable subgrain boundaries [16, 17].

The effect (i) could be observed in the region of Coble creep or Nabarro–Herring creep*. Also

*The strain rate in Nabarro–Herring creep region is too small to carry out creep tests.

0022–2461/84 $03.00 + .12

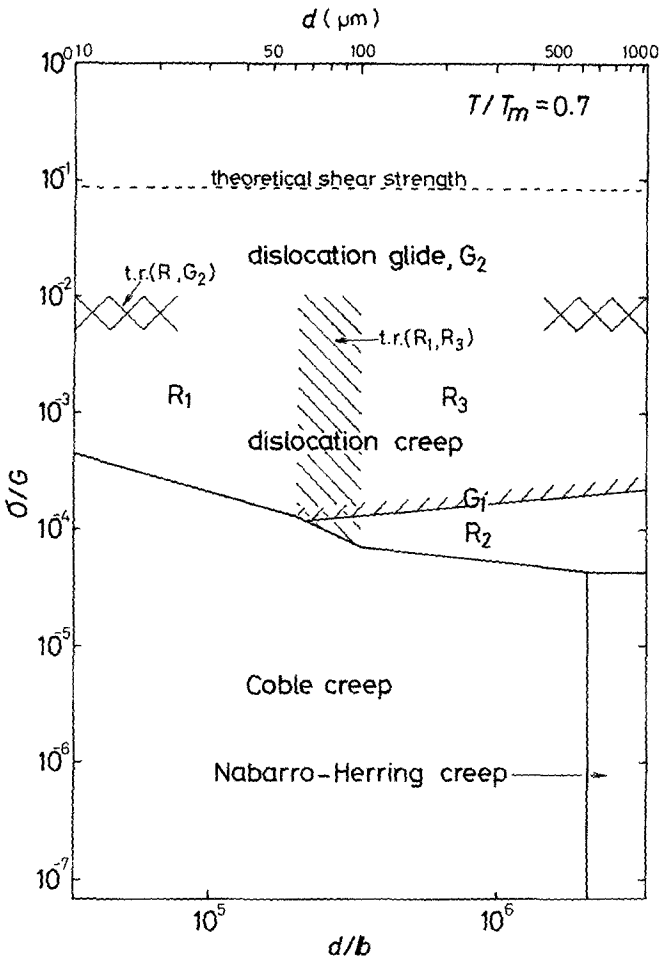

Figure 1 A $(\sigma/G) - (d/b)$ diagram for $T/T_m = 0.7$.

the effect (ii) is likely to be observed in domain R_1 and the effect (iii) in domain R_3. The condition of creep tests performed in the present study are as follows.

1. Creep stresses, σ, were in the range of 1.0 ~ 50.0 MPa, which is equivalent to the normalized stress range of $\sigma/G \simeq 2.1 \times 10^{-5} \sim 1.0 \times 10^{-3}$.

2. Creep temperatures, T, were around $0.7\,T_m$, i.e. $T = 1153 \sim 1213$ K.

3. Grain sizes, d, were in the range of 30 ~ 600 μm (the normalized grain size, $d/b \simeq 1.0 \times 10^5 \sim 2.0 \times 10^6$).

3. Materials and experimental procedure

The chemical composition is shown in Table I, together with that of an austenitic stainless steel without antimony. The steels were made by vacuum melting (~ 10^{-2} Pa).

Specimens of diameter 2.0 mm and gauge length 40 mm were prepared from the steels as detailed in previous work [18]. Primary heat treatments under various conditions resulted in a variety of grain sizes. A secondary heat treatment was performed in vacuum (~ 0.1 Pa) at test temperature for about 55 ksec, followed by an air cool. Creep tests were carried out in air after prior heating to 3.6 ksec at the test temperature.

4. Experimental results and discussion

The following equation is usually applied to the steady state creep rates.

$$\dot{\varepsilon}_s = A\sigma^n d^p \exp(-Q_c/RT) \qquad (1)$$

where A is a constant, n the stress exponent, p the grain size exponent, Q_c an activation energy of creep, and R is the gas constant.

TABLE I Chemical compositions (wt %) of the vacuum melted stainless steels

Vacuum melted stainless steels	Compositions			
	Cr	Ni	C	Sb
Sb-addition	23.20	22.64	0.005	0.40
Sb-free	22.77	21.39	0.005	Nil

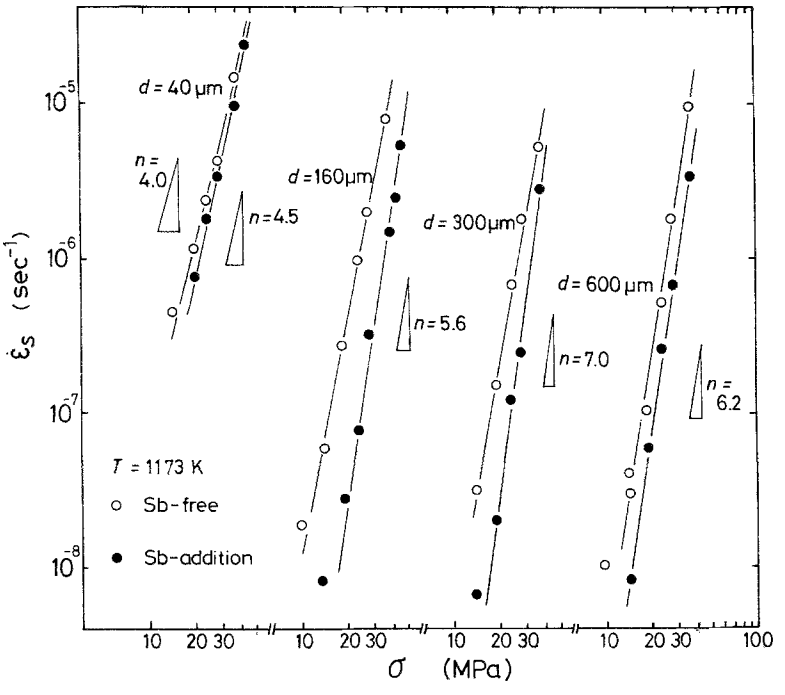

Figure 2 Stress dependences of the steady state creep rates, $\dot{\epsilon}_s$.

4.1. The effect of antimony additions in the region of dislocation creep

Fig. 2 shows the stress dependences of $\dot{\epsilon}_s$. The results for $d \simeq 40\,\mu m$ (fine grained specimens) reflect the influence of antimony on domain R_1 (cf. Fig. 1). Those of $d > 100\,\mu m$ are appropriate to domain R_3. It appears that domain R_1 is relatively less affected than domain R_3. However, antimony has the effect of reducing $\dot{\epsilon}_s$ over all grain sizes. The effect is enhanced with decreasing stress and leads to the n values higher than those of the Sb-free steel.

Fig. 3 shows the grain size dependences of $\dot{\epsilon}_s$. The effect of an antimony addition is most striking for the intermediate grain sizes ($d = 100 \sim 300\,\mu m$) but diminishes with decreasing grain size. It is interesting to note the strong effect in domain R_3, where the creep mechanism is strongly associated with dislocation substructure formation [16–18].

Fig. 4 shows the apparent activation energy, Q_c, for creep as a function of grain size. The values for the fine grained specimens are roughly equivalent to the activation energy, Q_v, for volume self-diffusion of iron ($\simeq 285\,kJ\,mol^{-1}$). On the other hand, those of the middle and coarse grained specimens have higher values than Q_v. These results may be explained in terms of the variation of "the internal stress" with temperature as reported in our previous papers [17, 18].

There are, however, two difficulties in interpreting the results in Figs. 3 and 4 for the purpose of understanding the segregation effect more clearly. The first concerns the antimony content per unit area of grain boundary. This concentration will be reduced with increasing temperature and may thus intensify the temperature dependence of $\dot{\epsilon}_s$. The second concerns the solubility. Grain boundaries and dislocations within substructures may be saturated by antimony atoms and other impurities. In fact, the stainless steel with antimony had grain boundary precipitates, although the steel without antimony had none. It appeared that the precipitates increased in both number and volume with decreasing temperature and increasing grain size.* It is considered that some of the antimony segregates to grain boundaries and subboundaries as second phase [5, 6]. Other antimony atoms segregate in solution to these boundaries, or exist in solid-solution in bulk. The Sb-segregation to substructures may lead to stabilization by dislocation locking [13]. On the other hand, the second phase on the grain boundaries can immobilize grain boundary dislocations.

*The precipitates increased insignificantly during creep, indicating that the secondary heat treatment before creep tests led to an equilibrium condition.

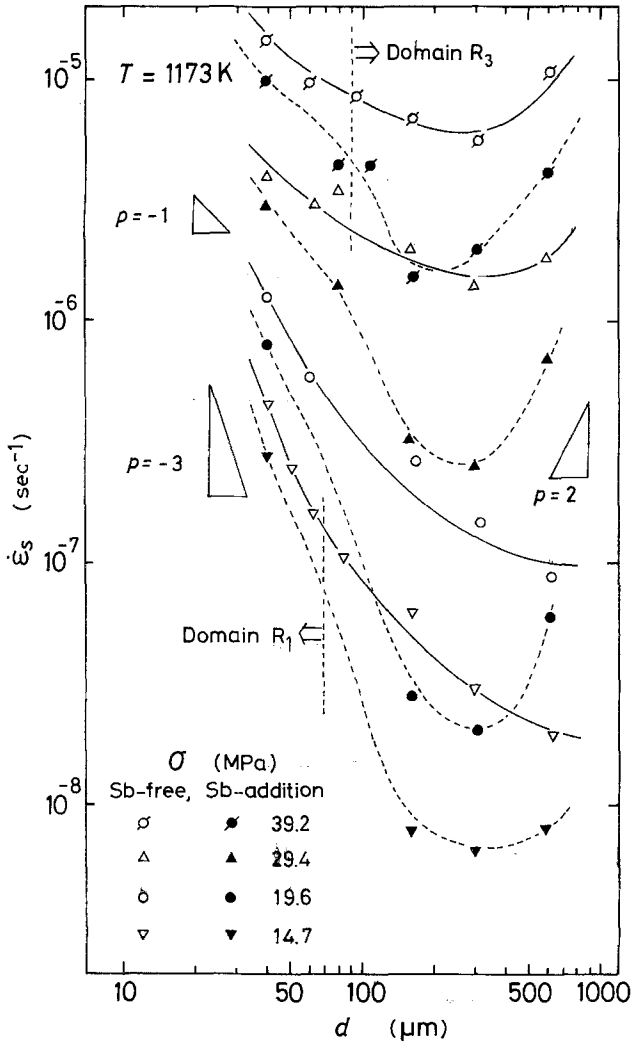

Figure 3 Grain-size dependences of the steady state creep rates, $\dot{\epsilon}_s$.

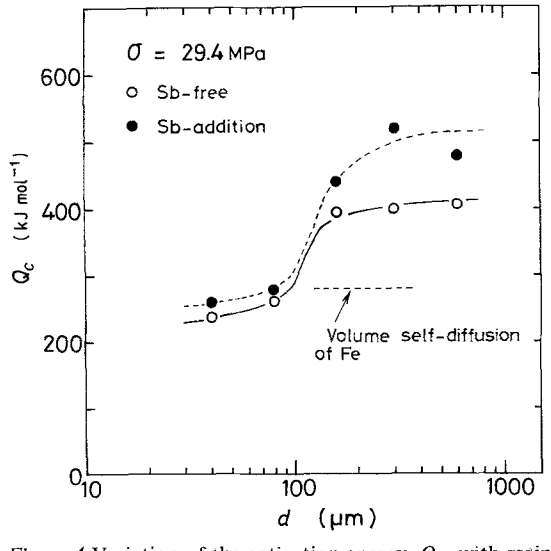

Figure 4 Variation of the activation energy, Q_c, with grain size.

4.2. The effect of antimony addition on Coble creep

The creep rate, $\dot{\epsilon}_s$, due to Coble creep can theoretically be impressed by

$$\dot{\epsilon}_s = 14\left(\frac{\pi\Omega\delta D_b}{kT}\right)(1/d)^3\sigma \qquad (2)$$

where Ω is the atomic volume, δ the grain boundary width, D_b the effective grain boundary diffusion coefficient, k Boltzman's constant, and the other parameters (T, d and σ) are designated above [19]. If D_b is assumed as that of iron, it could simply be given by $D_b = D_{b0}\exp(-Q_b/RT)$ where D_{b0} is the frequency factor and Q_b is the activation energy for the grain boundary self-diffusion of iron ($\simeq 180\,\mathrm{kJ\,mol^{-1}}$). Equation 2 is appropriate if the threshold stress, σ_t, is small enough to be negligible in comparison to the

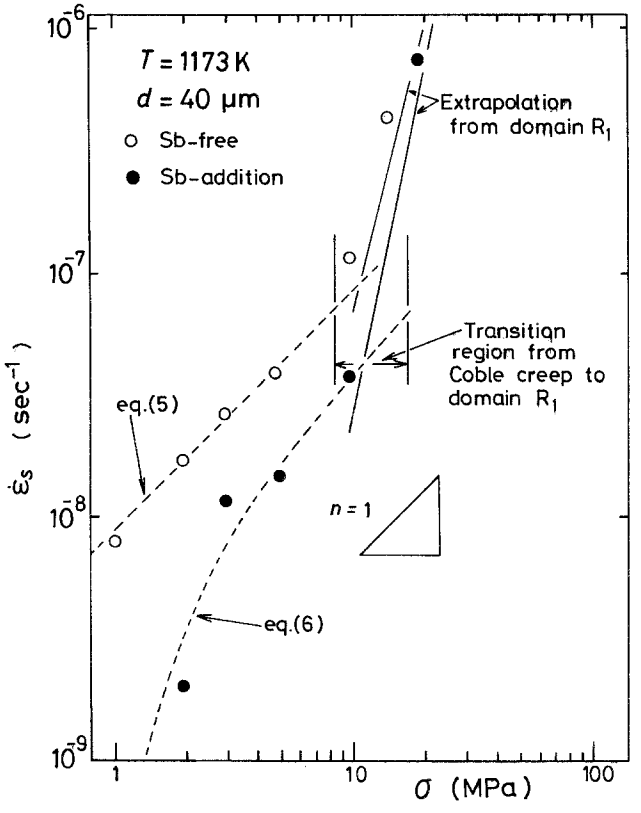

Figure 5 Stress dependences of the steady state creep rates, $\dot{\epsilon}_s$, in Coble creep region.

applied stress, σ [15, 19]. If it cannot be neglected, Bingham behaviour is exhibited [9–12], i.e. the steady state creep rate must be represented by

$$\dot{\epsilon}_s = K(\sigma - \sigma_t), \tag{3}$$

where K is given by

$$K = 14\left(\frac{\pi\Omega\delta D_{b0}}{kT}\right)(1/d)^3 \exp(-Q_b/RT). \tag{4}$$

Fig. 5 shows the stress dependence of $\dot{\epsilon}_s$ under the condition of Coble creep (see Fig. 1), using a log–log diagram. The steel doped with antimony does not show the n value equal to unity as required by Equation 1. It appears that antimony inhibits Coble creep by segregating to grain boundaries. Fig. 6 indicates that the addition of antimony amplifies Bingham behaviour. The parameter, K, and the threshold stress, σ_t, in Equation 3 can be

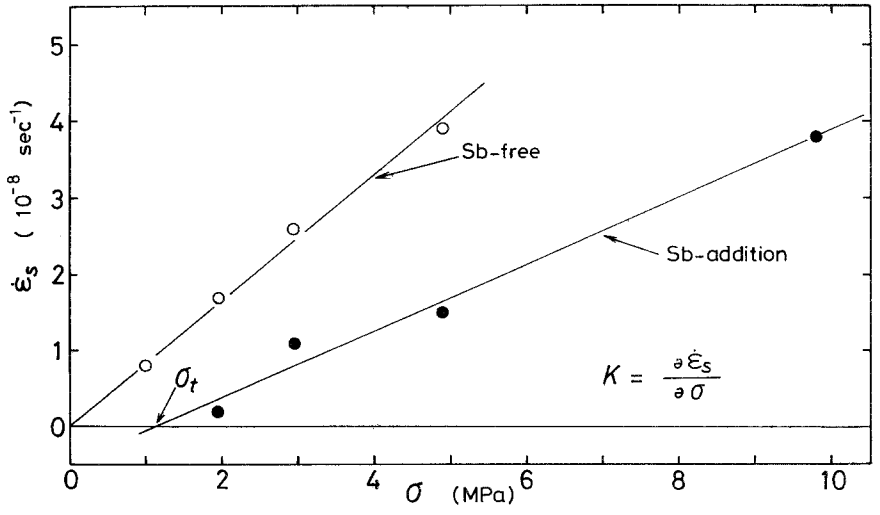

Figure 6 Variation of creep rate with stress. This is the figure in order to determine the threshold stress, σ_t.

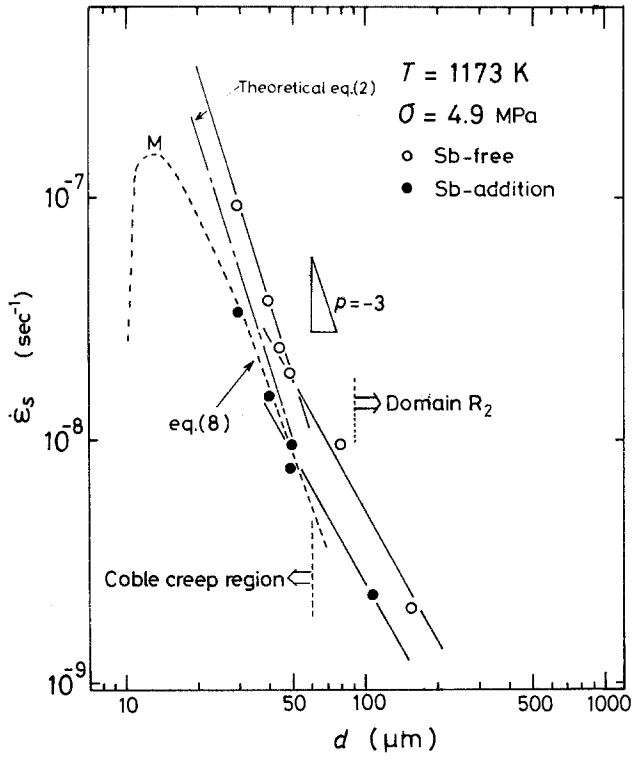

Figure 7 Grain-size dependences of the steady state creep rates, $\dot{\epsilon}_s$. Diffusional creep is replaced by dislocation creep, with increasing grain size, d. The ditted line of Equation 8 has a maximum point, M. This does not mean "no creep deformation" below it, but only the transition of creep mechanism from Coble creep to others unknown. It is, however, impossible in this temperature range to make small grain sizes ($d < 30\,\mu m$) stable during creep.

determined from this figure [9, 12]. The parameter, K, is reduced by the antimony addition because it is expected that the effective grain boundary width, δ, and the frequency factor, D_{b0}, are reduced by the segregation of antimony to grain boundaries.

The following relationships describe the curves in Fig. 5.

For the steel without antimony;

$$\dot{\epsilon}_s = 8.1 \times 10^{-9} \sigma \tag{5}$$

For the steel with antimony;

$$\dot{\epsilon}_s = 4.4 \times 10^{-9} (\sigma - 1.2). \tag{6}$$

Here the units of stress and strain rate are (MPa) and (sec^{-1}), respectively. The two curves are replaced by the constitutive equations of domain R_1 with increasing stress.

The threshold stress, σ_t, is usually expressed by

$$\sigma_t = \alpha_1 (Gb/d) \exp\left(\alpha_2 \frac{T_m}{T}\right) \tag{7}$$

where α_1 and α_2 are constants and the other parameters have been designated above [9, 12]. Substituting Equations 4 and 7 into Equation 3 and putting $\alpha_1 Gb \exp(\alpha_2 T_m/T)$ into $\Gamma(T)$, the following equation is obtained:

$$\dot{\epsilon}_s = \frac{A_0}{kT} (1/d)^3 [\sigma - \Gamma(T)/d] \exp(-Q_b/RT) \tag{8}$$

where A_0 is a constant. Equation 8 has been drawn by a dotted line in Fig. 7. It is indicated from Figs. 5 to 7 that the results for the steel with antimony can be explained by Equation 8. This is also supported by Fig. 8 which shows Arrhenius plots of $\dot{\epsilon}_s$ in the Coble creep region. The Sb-free stainless steel shows an activation energy of about 190 kJ mol^{-1}, which is roughly equal to that of grain boundary self-diffusion of iron. On the contrary, the steel doped with antimony show an activation energy of about 250 kJ mol^{-1}. Such a high value in Coble creep region has been observed in other stainless steels [8, 12]. The enlargement of Q_c can be understood by the temperature dependence of the threshold stress (Equations 7 and 8).

The decrease in the threshold stress with increasing temperature may be expected, because antimony atoms sugregate less to grain boundaries with increasing temperature [14].

5. Conclusions

1. The steady state creep rates of austenitic 25 wt % Cr–20 wt % Ni stainless steel are reduced by antimony additions.

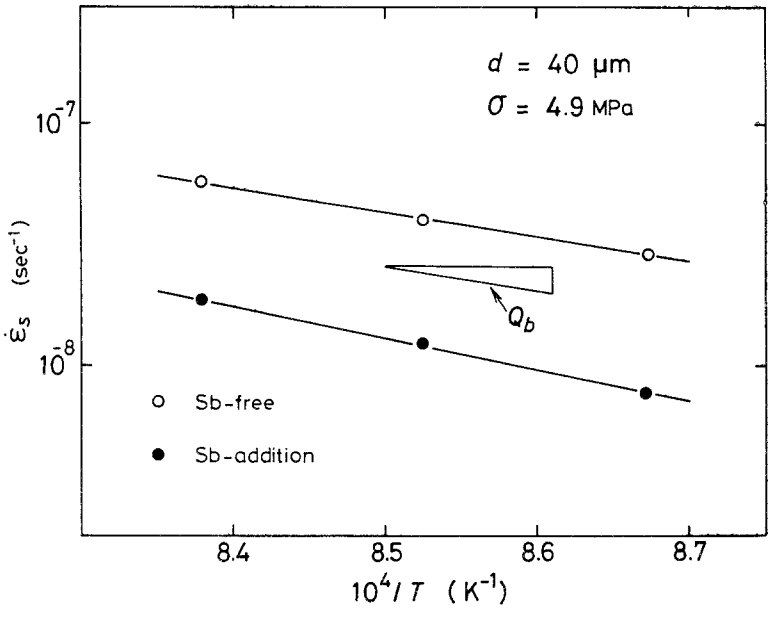

Figure 8 Variation of the activation energy, Q_c, for creep with grain size, d. This is in the range of diffusional creep region.

2. The reduction in $\dot{\varepsilon}_s$ can be understood in terms of the segregation of antimony to grain boundaries and substructures.

3. In the dislocation creep region, the effect of antimony addition is most striking in the intermediate grain size range ($d = 100 \sim 300\,\mu m$). The effect is more pronounced with decreasing stress.

4. In the Coble creep region, the effect is particularly remarkable. The threshold stress, σ_t, is increased by the antimony additions, i.e. Bingham behaviour ($\dot{\varepsilon}_s \propto \sigma - \sigma_t$) is observed.

Acknowledgement

This work is supported financially by The General Sekiyu Research and Development Encouragement and Assistance Foundation.

References

1. J. KAMEDA and C. J. MCMAHON Jr, *Met. Trans.* **11A** (1980) 91.
2. H. OHTANI, H. C. FENG, C. J. MCMAHON Jr and R. A. MULFORD, *ibid.* **7A** (1976) 87.
3. T. OGURA, C. J. MCMAHON Jr, H. C. FENG and V. VITEK, *Acta Metall.* **26** (1978) 1317.
4. A. JOSHI, *Scripta Metall.* **9** (1975) 251.
5. H. SUDO and H. TAKEZAWA, *J. Jpn. Inst. Met.* **41** (1977) 1166.
6. M. MAURER and M. C. CADEVILLE, *Phil. Mag.* **38A** (1978) 739.
7. F. GAROFALO, W. F. DOMIS and F. VON GEMMINGEN, *Trans. AIME* **230** (1964) 1460.
8. J. O. NILSSON, P. R. HOWELL and G. L. DUNLOP, *Acta Metall.* **27** (1979) 179.
9. B. BURTON, "In Vacancies 76", edited by E. Smallman and J. E. Harries (The Metal Society, London, 1977) p. 156.
10. I. G. CROSSLAND and B. D. CLAY, *Acta Metall.* **25** (1977) 929.
11. T. SRITHARAN and H. JONES, *ibid.* **27** (1979) 1293.
12. *Idem, ibid,* **28** (1980) 1633.
13. W. M. YIM and N. J. GRANT, *Trans. AIME* **227** (1963) 868.
14. D. MCLEAN, "Grain Boundaries in Metals" (Oxford University Press, London, 1957) p. 126.
15. Y. TAKAHASHI and T. YAMANE, *J. Mater. Sci.* **16** (1981) 3171.
16. *Idem, Scripta Metall.* **16** (1982) 1137.
17. *Idem, J. Mater. Sci.* **16** (1981) 397.
18. Y. TAKAHASHI, K. NAKAGAWA and T. YAMANE, *Z. Metallk.* **71** (1980) 572.
19. M. F. ASHBY and R. A. VERRALL, *Acta Metall.* **21** (1973) 149.

Received 15 March
and accepted 18 May 1983